



# Thymus-derived B cell clones persist in the circulation after thymectomy in myasthenia gravis

Ruoyi Jiang<sup>a</sup>, Kenneth B. Hoehn<sup>b</sup>, Casey S. Lee<sup>c</sup>, Minh C. Pham<sup>a</sup>, Robert J. Homer<sup>b,d</sup>, Frank C. Detterbeck<sup>e</sup>, Inmaculada Aban<sup>f</sup>, Leslie Jacobson<sup>g</sup>, Angela Vincent<sup>g</sup>, Richard J. Nowak<sup>c</sup>, Henry J. Kaminski<sup>h</sup>, Steven H. Kleinstein<sup>a,b,i,1,2</sup>, and Kevin C. O'Connor<sup>a,c,1,2</sup>

<sup>a</sup>Department of Immunobiology, Yale University School of Medicine, New Haven, CT 06511; <sup>b</sup>Department of Pathology, Yale University School of Medicine, New Haven, CT 06511; <sup>c</sup>Department of Neurology, Yale University School of Medicine, New Haven, CT 06511; <sup>d</sup>Pathology & Laboratory Medicine Service, VA CT Health Care System, West Haven, CT 06516; <sup>e</sup>Department of Surgery, Yale University School of Medicine, New Haven, CT 06511; <sup>f</sup>Department of Biostatistics, University of Alabama, Birmingham, AL 35294; <sup>g</sup>Nuffield Department of Clinical Neurosciences, John Radcliffe Hospital, University of Oxford, OX1 2JD Oxford, United Kingdom; <sup>h</sup>Department of Neurology, The George Washington University, Washington, DC 20052; and <sup>i</sup>Interdepartmental Program in Computational Biology & Bioinformatics, Yale University, New Haven, CT 06511

Edited by Lawrence Steinman, Stanford University School of Medicine, Stanford, CA, and approved September 28, 2020 (received for review April 15, 2020)

**Myasthenia gravis (MG) is a neuromuscular, autoimmune disease caused by autoantibodies that target postsynaptic proteins, primarily the acetylcholine receptor (AChR) and inhibit signaling at the neuromuscular junction. The majority of patients under 50 y with AChR autoantibody MG have thymic lymphofollicular hyperplasia. The MG thymus is a reservoir of plasma cells that secrete disease-causing AChR autoantibodies and although thymectomy improves clinical scores, many patients fail to achieve complete stable remission without additional immunosuppressive treatments. We speculate that thymus-associated B cells and plasma cells persist in the circulation after thymectomy and that their persistence could explain incomplete responses to resection. We studied patients enrolled in a randomized clinical trial and used complementary modalities of B cell repertoire sequencing to characterize the thymus B cell repertoire and identify B cell clones that resided in the thymus and circulation before and 12 mo after thymectomy. Thymus-associated B cell clones were detected in the circulation by both mRNA-based and genomic DNA-based sequencing. These antigen-experienced B cells persisted in the circulation after thymectomy. Many circulating thymus-associated B cell clones were inferred to have originated and initially matured in the thymus before emigration from the thymus to the circulation. The persistence of thymus-associated B cells correlated with less favorable changes in clinical symptom measures, steroid dose required to manage symptoms, and marginal changes in AChR autoantibody titer. This investigation indicates that the diminished clinical response to thymectomy is related to persistent circulating thymus-associated B cell clones.**

myasthenia gravis | thymectomy | B cells | autoimmune disease | adaptive immune cell receptor repertoire sequencing

**M**yasthenia gravis (MG) is a neuromuscular disorder caused by autoantibodies targeting components of the neuromuscular junction. Patients with MG experience skeletal muscle weakness, worsened by activity (1, 2). In upwards of 85% of MG patients, autoantibodies specifically target the nicotinic acetylcholine receptor (AChR) (2). Many clinical and experimental studies, including maternal-to-fetal transfer, plasma exchange to deplete antibodies, and passive transfer of patient-derived immunoglobulin show that AChR autoantibodies are demonstrably pathogenic (1, 3–10). AChR-mediated signal transmission is impaired by a number of autoantibody-mediated functions. AChR autoantibodies are predominantly IgG1 and IgG3, two subclasses that effectively activate complement (11–13). Thus, complement-mediated tissue injury and consequent removal of AChR from the muscle membrane represents a major mechanism of immunopathology. Additional mechanisms include autoantibody-mediated antigen cross-linking, resulting in internalization of AChR (by modulating autoantibodies), and a direct blocking of the acetylcholine binding site by the autoantibodies (14–19).

A key source of these pathogenic AChR autoantibodies in MG patients is the MG thymus. Thymic lymphofollicular hyperplasia (20) with germinal centers is observed in ~70% of younger MG patients (21). The thymus in these patients contains both AChR-specific IgG (22) and B cells (10) that can secrete these autoantibodies (23). Transplantation of thymus from AChR-MG patients into immunodeficient mice results in human AChR-specific autoantibody deposits at the neuromuscular junction, and subsequent manifestation of MG-like symptoms (24). Thymus-associated plasma cells and plasmablasts spontaneously produce AChR autoantibodies in vitro (25, 26) and activated memory B cell populations (27–29). B cells residing in the hyperplastic thymus organize within tertiary lymphoid organs,

## Significance

**Myasthenia gravis is caused by autoantibodies, which target postsynaptic proteins, primarily the acetylcholine receptor, that inhibit neuromuscular signaling. The myasthenia gravis thymus can serve as a reservoir of acetylcholine receptor-specific autoantibody-producing B cells. Thus, thymectomy is provided as a treatment. However, many patients fail to improve; the causes of poor responses are not understood. This investigation demonstrated that disease-associated B cell clones mature in the thymus before emigrating to the circulation. These B cell clones are present in the circulation after thymectomy and their persistence correlated with less favorable changes in clinical symptoms after thymectomy. This investigation provides mechanistic insight into the immunopathology associated with a diminished clinical response to thymectomy.**

Author contributions: H.J.K., S.H.K., and K.C.O. designed research; R.J., K.B.H., C.S.L., M.C.P., R.J.H., F.C.D., L.J., A.V., R.J.N., and H.J.K. performed research; K.B.H. and S.H.K. contributed new reagents/analytic tools; R.J., K.B.H., I.A., A.V., R.J.N., and H.J.K. analyzed data; and R.J., S.H.K., and K.C.O. wrote the paper.

Competing interest statement: K.C.O. has received research support from Ra Pharma and is a consultant and equity shareholder of Cabaletta Bio. K.C.O. is the recipient of a sponsored research subaward from the University of Pennsylvania, the primary financial sponsor of which is Cabaletta Bio. S.H.K. receives consulting fees from Northrop Grumman. R.J.N. has received research support from Alexion Pharmaceuticals, Genentech, Grifols, and Ra Pharma. H.J.K. has served as an advisor to Alnylam Pharmaceuticals, Ra Pharmaceuticals, and UCB Pharmaceuticals, and is Chief Executive Officer and Chief Marketing Officer of ARC Biotechnology, LLC, based on US Patent 8,961,98.

This article is a PNAS Direct Submission.

Published under the PNAS license.

See online for related content such as Commentaries.

<sup>1</sup>S.H.K. and K.C.O. contributed equally to this work.

<sup>2</sup>To whom correspondence may be addressed. Email: steven.kleinstein@yale.edu or kevin.oconnor@yale.edu.

This article contains supporting information online at <https://www.pnas.org/lookup/suppl/doi:10.1073/pnas.2007206117/-DCSupplemental>.

First published November 16, 2020.

forming structures that share many characteristics associated with germinal centers (30–33). The presence and frequency of these structures positively associates with the presence of circulating AChR autoantibodies (34). Expanded clones among the MG thymus resident B cells is consistent with the presence of ongoing germinal center-based maturation processes (35, 36). These clones feature the characteristics of antigen experience, including isotype class switching, somatic hypermutation, and biased usage of antibody variable region gene segments (35, 37–40).

These collective studies clearly demonstrate that the thymus plays a fundamental role in the production of AChR autoantibodies and consequently the immunopathology of MG. Based only on empiric clinical evidence, thymectomy (TX) had already been widely used as a long-standing treatment strategy for AChR autoantibody-positive MG (41). A multicenter, single-blind, randomized clinical trial (MGTX) designed to evaluate the efficacy of thymectomy plus prednisone versus prednisone alone in generalized nonthymomatous AChR-MG was recently performed to formally test the effect of thymectomy (42). The study demonstrated the efficacy of thymectomy as the procedure led to a significant improvement in muscle weakness, decreased steroid usage, and decreased frequency of rehospitalization over the course of 3 y. Results from a 2-y extension study of the MGTX trial (43) demonstrated that the patients who underwent thymectomy were more likely to have a better clinical status compared to patients who were treated with prednisone alone. Moreover, therapeutic effects from thymectomy continue to be observed years after the procedure, but some patients experienced more benefit than others. These findings are consistent with other studies, which showed rates of complete stable remission in only 40 to 50% of patients when followed for years after the procedure (44, 45). Furthermore, the AChR autoantibody titer decreases in the majority of those treated by thymectomy, but almost never reaches undetectable levels (34, 46) and only modestly decreases in many (47). Understanding both the mechanistic basis for heterogeneous responses and why thymectomy does not consistently lead to complete stable remission is therefore critical to improving the management of AChR autoantibody-positive MG patients with thymic lymphofollicular hyperplasia.

Given extensive evidence that disease-causing B cells in AChR-MG are found in the thymus alongside clinical evidence showing heterogeneous responses to thymectomy, we sought to test the possibility that B cell clones from the thymus persist in the periphery after removal of the thymus. We hypothesized that B cell clones from the thymus would be found in the circulation and that the persistence of these clones overall would correlate with disease persistence. Thus, in this study, we test the hypothesis that the global depletion of B cell clones from the thymus, including those that produce AChR autoantibodies, is a mechanism by which thymectomy reduces disease burden. To test this hypothesis, we performed adaptive immune receptor repertoire (AIRR) sequencing (AIRR-seq) of B cell receptor (BCR) repertoires from the thymus and paired longitudinal peripheral blood samples from the MGTX trial and an independent center, generating approximately half a million V(D)J sequences in total. AIRR-seq has the capacity and depth to identify rare sequences in the large ( $10^{11}$  B cells) circulating peripheral repertoire found in humans (48). Consequently, this approach allowed us to identify rare B cell clones in the circulation related to those in the thymus and track their frequency over time after thymectomy.

## Materials and Methods

**Study Design and Approval.** Subjects were selected at random from the total of 82 MGTX subjects who completed the trial and provided biological samples. Subjects without adequate thymic tissue or whole-blood DNA/RNA samples for analysis were excluded, then substitutes were randomly selected. The National Institute of Neurological Disorders and Stroke funded

the trial and assembled a Data Safety Monitoring Board to independently monitor study activities. Sites received local institutional review board/ethics committee approvals, and each patient provided written informed consent before study entry, including provision of specimens. Stored biological specimens from the selected MGTX subjects were then deidentified and provided for the present study. An additional thymus specimen and matched peripheral blood mononuclear cells (PBMCs) were collected from a patient who underwent thymectomy at Yale New Haven Hospital and was treated at the Yale Myasthenia Gravis Clinic. This patient and these specimens were not affiliated with the MGTX trial. Written informed consent was provided. Tissue and PBMCs were retrieved from an existing biorepository for use in the current study. The overall study was approved by Yale University's Institutional Review Board. Clinical and demographic information for the entire study cohort are provided (Table 1).

**Radioimmunoprecipitation Assay for AChR Autoantibody Levels.** AChR autoantibody levels for the MGTX trial specimens were measured by radioimmunoprecipitation assay (RSR Ltd.) (46). A serum concentration was chosen for each patient baseline sample, which immunoprecipitated ~40 to 50% of the total, and that concentration was used for each of the samples from that patient. Titers were expressed as nanomoles precipitated by a liter of serum. For assessing changes over time, the percent change in titer for each patient was used rather than the actual titer. The AChR autoantibody levels for specimens from patient THY-Y were measured by radioimmunoprecipitation assay performed at the Mayo Clinical Laboratories, (Rochester, MN), using a reference range positive  $>0.02$  nmol/L.

**Isolation of Thymus Genomic DNA and RNA for AIRR-Seq.** Thymus regions were selected for sequencing based on the presence of B cell-enriched germinal center-like structures, the presence of which was confirmed through tissue section histology and immunohistochemistry. Thymus blocks from the MGTX trial were mounted and frozen in OCT. Sections were then isolated and assessed for the presence of such structures by staining with H&E and a mouse anti-human CD23 antibody (clone M-L233, BD Pharmingen catalog number 555707), as per the manufacturer's instructions. Once a region was confirmed to include a B cell-enriched germinal center-like structure, adjacent tissue slices were collected and immediately placed in RLT lysis buffer for RNA extraction using the Qiagen RNA Mini kit per manufacturer's instructions. For mRNA-based sequencing, approximately 10 contiguous 10- $\mu$ m slices were extracted from each block. Genomic DNA (gDNA) was isolated in a similar manner, except that sections were immediately placed in lysis buffer using Qiagen's DNAeasy Blood and Tissue kit per the manufacturer's instructions. For the patient not associated with the MGTX trial, sections were collected and mRNA was isolated for sequencing using methods similar to those described for MGTX specimens, except only H&E staining was performed to confirm the presence of a lymphocytic infiltrate. In addition, adjacent, formalin-fixed paraffin-embedded thymus blocks, from this patient, were available. Sections were stained with an anti-CD20 monoclonal antibody (clone L26, Dako/Agilent catalog number M0755), as per the manufacturer's instructions.

**BCR Library Preparation.** For gDNA-derived BCR libraries, BCR CDR3 regions were amplified and sequenced using the ImmunoSeq assay, which involves a multiplexed PCR using forward primers specific to VH gene segments (located in the FR3 region) and reverse primers specific to the BCR JH gene segments (Adaptive Biotechnologies). RNA-derived BCR libraries were prepared using the NEBNext Immune Sequencing Kit (Human) reagents provided by New England Biolabs (Eileen Dimalanta and Chen Song, New England Biolabs, Ipswich, MA) using methods we previously described (49). Briefly, the RNA was reverse-transcribed into cDNA using a biotinylated oligo dT primer. An adaptor sequence, containing a universal priming site and a 17-nucleotide unique molecular identifier (UMI) was added to the 3' end of all cDNA. Following purification using streptavidin-coated magnetic beads, PCR was performed to enrich for immunoglobulin sequences using a pool of primers targeting the IGHA, IGHD, IGHE, IGHG, IGHM, IGKC, and IGLC regions. This immunoglobulin-specific primer pool contained sequences with a priming site for a secondary PCR step. The second primer in this reaction is specific to the adaptor sequence added during the reverse transcription step, and contains a sample index for downstream pooling of samples prior to sequencing. Following purification of PCR products using AMPure XP beads, a secondary PCR was performed in order to add the full-length Illumina P5 Adaptor sequence to the end of each immunoglobulin amplicon. The number of secondary PCR cycles was tailored to each sample to avoid entering plateau phase, as judged by a prior quantitative PCR analysis. Final products were purified, quantified with a TapeStation (Agilent Genomics) and pooled in equimolar

**Table 1. Demographic and clinical information of study patients at the time of thymectomy**

Patient ID, gender, age (y)	MGFA class at TX	Disease duration at TX (y)	Prednisone at TX (mg/d)	Prednisone 1 y average (mg/d)	Prednisone 2-y average (mg/d)	AChR-Ab at TX	AChR-Ab at 1 y	AChR-Ab at 2 y
THY1 F, 20	IIb	2.4	40	49.2	38.6	41.14	51.28	62.10
THY2, F 19	III	0.4	10	45.4	34.4	31.60	27.996	29.70
THY3, F, 19	IIb	0.6	0	36.6	17.6	36.36	28.24	26.61
THY4, F, 18	IIa	1.9	30	48.5	35.1	12.66	15.636	13.35
THY5, F, 46	IIa	0.9	0	35.9	35.9	112.60	36.08	43.24
THY6, M, 24	IIb	1.1	50	61.9	40.7	28.57	29.864	23.70
THY7, F, 22	IIa	0.7	25	37.1	18.5	No data	No data	No data
THY8, F, 21	III	0.7	38	60.9	32.3	165	367.76	327.64
THY-Y, F, 36	IIb	2.8	20	Non-MGTX	Non-MGTX	0.22	0.25*	Non-MGTX

F, female; M, male; TX, thymectomy. AChR-Ab titers are given in nanomolar units (nM).  
\*AChR antibody titers for patient outside MGTX trial were collected at baseline at 6 mo after thymectomy.

proportions, followed by sequencing with a 20% PhiX spike on the Illumina MiSeq platform according to manufacturer's recommendations, performing 325 cycles for read 1 and 275 cycles for read 2.

**Raw Read Quality Control and Assembly.** Preprocessing was carried out using PRESTO v0.5.4 (<https://presto.readthedocs.io/en/stable/>). Reads below a mean phred score of 20 and those without a constant region primer (above error rate of 0.2) or template switch sequence (above error rate of 0.5) were discarded. A UMI was assigned to each read by extracting the first 17 nucleotides following the template switch site. Multiple reads from the same UMI were aligned using MUSCLE v3.8.31 (50). Sequencing and multiplexing errors in the UMI region were then corrected using the following approach. Sequences with similar UMIs were clustered using the CD-HIT-EST algorithm v4.7 (51) by analyzing the distribution of pairwise sequence hamming distances; 10,000 UMI sequences were sampled and the threshold was identified as the minima between 1.0 (identical) and 0.25 (the expected hamming distance between two random sequences of 4 nucleotides). These groups of sequences were further clustered into smaller groups; the average distribution of pairwise sequence hamming distances across the non-UMI region of the sequence was computed for all groups. Sequences were then clustered using a threshold identified by an approach similar to that described above. If clusters of sequences spanned multiple multiplexed samples, they were assigned to the majority sample. Note that given limitations to the CD-HIT-EST algorithm, a threshold of 0.8 was used if the identified threshold was lower than 0.8. Reads from the same cluster were collapsed into a consensus sequence. Clusters with errors exceeding 0.1 or majority isotype that was less than 60% of the cluster were discarded. Mate-pairs were assembled into immunoglobulin sequences with a minimum overlap of 8 base pairs and maximum error of 0.3. Mate-pairs failing this assembly were assembled by alignment against the IMGT human germline IGHV reference database (IMGT/GENE-DB v3.1.19; retrieved June 21, 2018) with a minimum allowed identity of 0.5 and a E-value threshold of  $1 \times 10^{-5}$  (49, 52). Isotypes were assigned by local alignment of the 3' end of assembled Ig sequences to known isotype-constant region sequences with a maximum tolerated mismatch of 0.4. Duplicate sequences were discarded except those assigned to different isotypes. Sequences represented by only a single reconstructed mate-pair sequence were discarded.

**V(D)J Gene Annotation, Sequence Filtering, Clonal Assignment, and Germline Reconstruction.** Following preprocessing, V(D)J germline genes were assigned with IgBLAST v1.7.0 (53) using the June 21, 2018 version of the IMGT gene database. Following V(D)J annotation, nonfunctional sequences were removed. Functional VH V(D)J sequences were assigned into clonal groups using Change-O v0.3.4 (54) as we have previously described (49). First, sequences were partitioned based on common IGHV gene annotations, IGHJ gene annotations, and junction lengths. In the case of genomic DNA-derived sequences, primer annotations were used to assign IGHV and IGHJ gene annotations. Within these larger groups, sequences differing from one another by a length normalized Hamming distance within the junction region were defined as clones by single-linkage clustering. The clonal distance threshold was determined by identifying the local minima between the two modes of a within-sample bimodal distance-to-nearest histogram (54); the final threshold chosen was the average threshold across all samples. Clones from these V(D)J sequences were identified by grouping sequences using identical VH and JH genes with a fraction of shared junctional nucleotides

less than a specified (7.7% for genomic DNA, 18.8% for RNA sequencing) threshold (*SI Appendix, Figs. S5 and S7*). Full-length germline sequences were reconstructed for each clonal cluster (VH) or sequence (VL) with D segment and N/P regions masked (replaced with Ns); any ambiguous gene assignments within clonal groups were resolved by majority rule.

**Analysis of Somatic Hypermutation, Selection Pressure, Lineage Trees, Diversity, and CDR3 Properties.** Mutations were detected relative to the germline sequence using SHazaM v0.1.8 in R v3.4.2 (55). A minimum threshold of six sequences associated with a sample was used to exclude comparisons of somatic hypermutation (SHM) involving samples with too few sequences. Selection strength of FWR and CDR regions was quantified using the BASELINE implementation in SHazaM (56). Analysis of CDR3 physiochemical properties was performed using Alakazam v0.2.11. Glycosylation sites were assessed by searching the translated VH gene after alignment (or germline reassembly) according to IMGT definitions for the regular expression pattern "[N<sup>A</sup>P][S,T]". Diversity analysis was performed using a generalized Hill index in Alakazam, with down-sampling (the number of sequences from the sample with the fewest sequences) and bootstrapping (1,000 replicates) from the inferred complete clonal abundance to account for variability in depth across samples (57). Clonal sharing was computed using a Bray-Curtis metric implemented by the function `scipy.spatial.distance.braycurtis(scipy.v1.1.0)` and log-transformed for assessing background significance. In this analysis, the average overlap in comparisons with the circulating repertoire of other subjects from the trial was computed (the background, "interpatient") relative to the overlap between the circulating and thymus repertoire from the same individual ("intra-patient"). The analysis of shared clones in the thymus and circulation was restricted to thymus samples with more than 5,100 isotype-switched V(D)J sequences given the importance of consistent sequencing depth for the identification of sharing and quantification of significance.

**Inference of B Cell Lineage Trees and Migration Analysis.** The goal of these analyses is to use B cell lineage trees to determine whether IgG sequences in the thymus were predicted to be the immediate ancestor to IgG sequences in the blood more frequently than expected by chance. To account for uncertainty in tree topology, the columns of each clone's multiple sequence alignment were sampled with replacement, forming bootstrap replicates. B cell lineage tree topologies and branch lengths were then estimated for each replicate using the *dnapars* program distributed as part of PHYLIP (v3.697) (58). An implementation of the Sankoff parsimony algorithm (59) with equal weights for switches among locations was then used to determine the set of internal node locations that resulted in the fewest number of location changes along the tree, given the sampling location of each sequence at the tree's tips. Clusters of internal nodes separated by zero length branches (polytomies), were reordered using nearest-neighbor interchange moves to minimize the number of changes along the tree and to appropriately represent possible directions of migration (60). For each bootstrap replicate, the proportion of predicted changes from the thymus to the circulation (switch proportion) was compared to the same statistic in trees where sample locations were randomized at the tips. The difference between these values ( $\delta$ ) was recorded, and this process was repeated for 1,000 bootstrap replicates. The *P* value for enrichment of changes from thymus to circulation (i.e.,  $\delta > 0$ ) is the proportion of replicates in which  $\delta \leq 0$ . If  $P < 0.05$  and  $\delta > 0$ , this indicates a significantly more biased ancestor/descendant relationship from thymus to circulation IgG than expected by

chance in the lineages surveyed. Only IgG sequences were included. Furthermore, only clones that contained at least one sequence from the thymus and circulation at the date of thymectomy and contained more than two sequences that were either distinct or found in different samples, were included. Clones found to be erroneous because they spanned multiple patients were excluded. Patients THY3, THY4, and THY8 had fewer than two clones each satisfying these criteria and were therefore not included in this analysis. These analyses were performed using the R package *dowser* v0.0.1 (60) and *IgPhyML* v1.1.3 (61).

**Statistical Analysis.** R v3.4.2 (55) and Python 3.5.4 (2017) was used for all statistical analysis. Dataframe handling and plotting was performed using functions from the *tidyverse* 1.2.1 in R and *pandas* 0.24.2, *scipy* 1.1.0 and *matplotlib* 2.2.2 in *python3*. All parametric statistical testing was performed in R using the *aov* function for two-way ANOVA or *t.test* functions for paired two-tailed Student *t* tests (or one-tailed Student *t* test where specified). A significance threshold of  $<0.05$  was used and shown on plots with a single asterisk; double asterisks correspond to a  $P < 0.01$  and triple asterisks correspond to a  $P < 0.001$ .

## Results

**Patients, Specimens, and Experimental Design.** Eight thymectomy-treated AChR-autoantibody-positive MG subjects (seven female, one male; mean age of 23.6 with SD of 9.2 y, range 18 to 46 y) from the MGTX trial (Table 1) were selected for study. Matched specimens from each patient included: 1) mRNA and genomic DNA from PBMCs, which were isolated at the time of the resection (referred to as baseline); 2) mRNA from PBMCs isolated 12 mo after the thymectomy; and 3) frozen intact thymus tissue specimens. In addition, a patient (female, age 36 y) who underwent thymectomy at an independent tertiary care facility unaffiliated with the MGTX trial was also included to assess the generalizability of our findings (Table 1). Matched specimens from this patient included mRNA from PBMCs, which was isolated at the time of the resection and also 6 mo after the thymectomy, and intact thymus tissue specimens. Thymus specimens from all subjects were sectioned and evaluated by histology and immunohistochemistry such that sections observed to contain morphological features resembling B cell-enriched germinal centers were specifically selected for sequencing (SI Appendix, Figs. S1 and S2). High-depth AIRR-seq was performed using complementary mRNA and gDNA-based approaches. Experiments were designed to test whether B cell clones in the thymus were shared among those in the circulation and how shared circulating clones behaved following thymectomy (SI Appendix, Fig. S3).

**MG Thymus Resident B Cells Feature Antigen-Driven Characteristics.** The repertoire of B cells that reside in tertiary lymphoid organs, which are often found in autoimmune tissue, have been observed to possess unique characteristics often associated with a developing response to specific antigens. These qualities include elevated frequency of class-switching, elevated SHM frequency, and lower replacement/silent mutation ratio: That is, increased signature of negative selection, elevated frequency of N-glycosylation sites, and reduced frequency of VH3 gene usage (62, 63). High-depth AIRR-seq has not been applied to investigate whether these features are consistently found in thymus from AChR-MG (AChR autoantibody-positive MG) patients where such tertiary lymphoid structures are present. Thus, we examined the thymus B cell receptor repertoire for the enrichment of these same features by performing mRNA-based AIRR-seq on the eight MGTX trial-derived thymus specimens (SI Appendix, Table S1) and paired repertoires from the circulation (derived from whole-blood RNA collected at baseline).

On average, the thymus B cell repertoire was 85.4% IgG switched compared to only 28.0% in the circulation (paired *t* test  $P = 1.3e-06$ ) (Fig. 1A). Correspondingly, the fraction of IgM and IgA switched V(D)J sequences in the thymus-derived B cell

repertoire was significantly lower (paired *t* test  $P = 1.3e-03$  and  $P = 4.4e-04$ , respectively). The average SHM frequency for IgM and IgA was not significantly different for thymus-derived B cells compared to those from the circulation. However, when restricting the analysis to IgG switched V(D)J sequences (given the clear role of this isotype in MG), a consistent elevation in SHM frequency for IgG-switched B cells in the thymus (6.3% mutated) was observed compared to the circulation (5.5% mutated; paired *t* test  $P = 0.039$ ) (Fig. 1B). In addition, we examined the ratio of replacement to silent mutations as this provides information about features of antigen selection not provided by quantification of total SHM frequency alone. Circulating and tissue-resident B cells from patients with autoimmunity (as well as in the context of vaccination) have consistently been observed to display a lower-than-expected ratio of replacement to silent mutations (61, 63–65). Negative selection pressure may favor the conservation of protein structure by introducing mutations that preserve antibody amino acid sequence; this may be a key feature of repertoires actively undergoing affinity maturation (61, 66). Thymus samples were observed to contain B cells with lower selection strength than sequences from circulating B cells ( $P = 1.0e-9$  for CDR,  $P = 4.3e-2$  for FWR regions) (Fig. 1C) (66).

Several recent studies have also demonstrated an enrichment of variable region N-linked glycosylation sites relative to healthy controls in B cells from the peripheral blood of patients with rheumatoid arthritis (62) or in the parotid gland of patients with primary Sjogren's syndrome, a structure also known to contain ectopic lymphoid follicles (63). Consistent with these observations, we found that the thymus IgG-switched BCR sequences were more enriched than paired blood for N-linked glycosylation DNA motifs, (frequency of 14.5% vs. 6.9%, respectively; paired *t* test  $P = 0.008$ ) (Fig. 1D). This frequency was also elevated for thymus IgM-expressing B cells but not for IgA (paired *t* test  $P = 0.037$  and  $P = 0.56$ , respectively). To investigate if the elevated frequency of N-linked glycosylation sites was introduced through affinity maturation, we assessed the frequency of these sites in the associated germline V genes and observed that a difference in N-linked glycosylation frequency could no longer be detected (paired *t* test  $P = 0.50$ ) for thymus IgG-expressing B cells, while the frequency for IgM was still elevated (paired *t* test  $P = 0.019$ ) (Fig. 1E). This result indicates that N-linked glycosylation sites were generated by affinity maturation and possibly due to antigen-driven selection for IgG-switched B cells. Finally, we sought to investigate if IgG-switched B cells in the thymus use a different set of V genes compared to those in the circulation. A significant difference in terms of V family usage (ANOVA  $P = 0.013$ ) (SI Appendix, Fig. S4A) was observed. Specifically, there was a decrease in the use of VH3 family genes and an increase in the usage of VH4 family genes in the thymus IgG-switched B cell repertoire.

Collectively, these findings demonstrate that the thymus is highly enriched for somatically mutated IgG-switched B cells with an elevated N-linked glycosylation site frequency, signatures of negative selection, and biased usage of VH4 V family genes compared to VH3 family genes. These are all features of mature antigen-driven B cells, including plasma cells, which are likely to be disease-relevant. Furthermore, these characteristics that are associated with an antigen-driven response are also found to be enriched, albeit to a lesser degree, in the circulating B cells of MG patients (65).

**Clonally Related B Cells Reside in Both the Thymus and Circulation.** We next sought to determine whether B cells present in MG thymus had clonal relatives in the circulation. We define a B cell clone as a set of V(D)J sequences that arise from a common immunoglobulin heavy chain (IGH) gene recombination event. Thus, V(D)J sequences belonging to a clone share common IGHV, IGHJ, and IGHD genes as well as a set of N/P additions

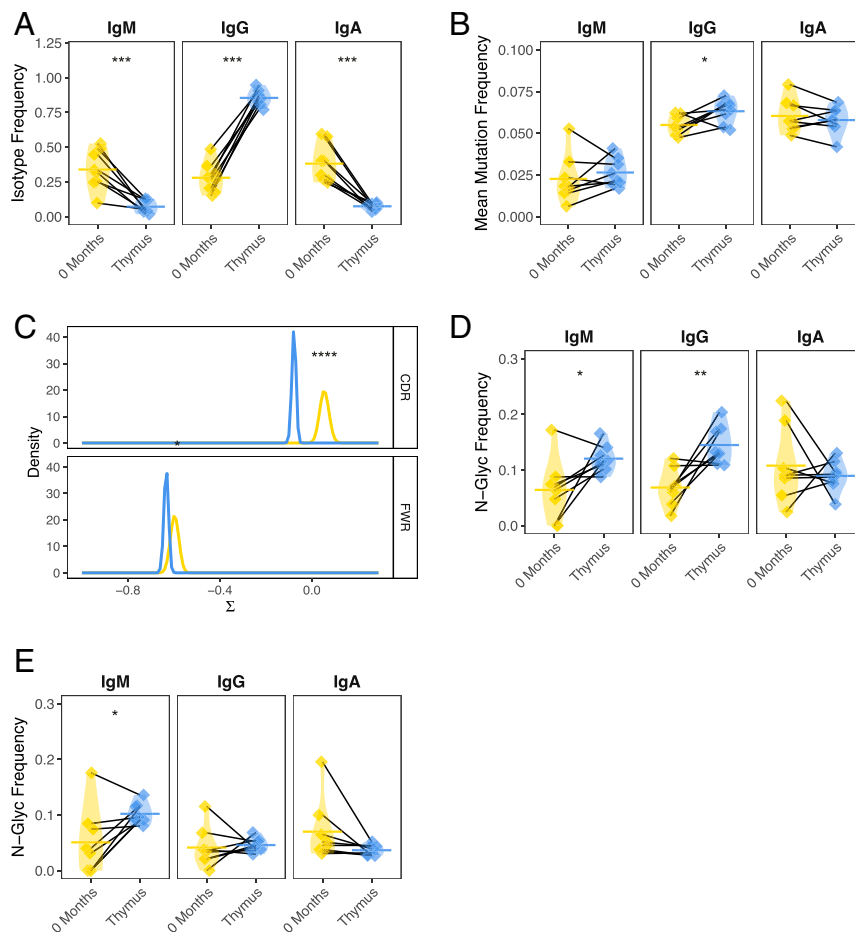


**Fig. 1.** The thymus-associated B cell repertoire is distinct from the paired circulating repertoire. AIRR-seq was performed to generate B cell repertoires for eight MGTX trial-derived thymus specimens and paired PBMCs collected at baseline. Key features of antigen-experience B cells in each of the respective repertoires were then compared. (A) Overall constant region (isotype) usage frequencies are quantified for thymus compared to the circulating compartment per patient. Horizontal bars show the average frequency of constant region usage across patients. Frequencies belonging to the same patient are paired with a black line. (B) Individual SHM frequencies for thymus compared to circulating B cells are presented. Horizontal bars show the average SHM frequency for a given sample status (i.e., thymus or circulation). Frequencies belonging to the same patient are paired with a black line. (C) BASELINE probability distribution functions (PDF) are shown for thymus and circulating repertoires, with density shown for a range of selection strengths ( $\Sigma$ ) on the x axis. PDFs were determined via convolution of subject-specific PDFs for each status to generate a single aggregate status. (D) Individual frequencies for the occurrence of glycosylation (N[X](S/T)) sites are quantified for thymus compared to circulating B cells and (E) for the inferred germline of these sequences. Horizontal bars show the average glycosylation frequency for a given cluster. Frequencies belonging to the same patient are paired with a black line. Statistical differences are shown only when significant (\*\*\*\* $P < 0.0001$ ; \*\*\* $P < 0.001$ ; \*\* $P < 0.01$ ; \* $P < 0.05$ ).

but may differ from each other due to sequence diversity introduced by SHM. A threshold (18.8%) was used to define how different junction sequences from the same clone could be among sequences sharing IGHV and IGHJ genes (SI Appendix, Fig. S5). It is possible that sequences from biologically distinct clones share sufficient sequence similarity to be incorrectly grouped into the same clone, however. To estimate the frequency at which clones are spuriously observed to be shared between the circulation and thymus, the average background sharing between the circulation and the thymus of unrelated individuals was calculated. This rate was used as a null distribution to establish the significance of the observed clonal sharing between the circulation and the thymus. Seven of the eight MGTX patients were studied, due to insufficient sequencing depth for clonal sharing analysis in one specimen (only 5,070 thymus sequences). In these seven patients, a mean of 482.9 clones (2.1% of all thymus clones) were found to be shared between the thymus and circulation at baseline, while a mean background of 90.6 clones (0.6% of all thymus clones) were found shared between the same two compartments of unrelated

individuals (SI Appendix, Fig. S6). The observed sharing was significantly higher than the background for all thymus tissue samples studied (one-tailed paired  $t$  test  $P = 5.4e-4$ ). That is, more thymus clones were shared with the circulation of the same individual, than that of unrelated individuals (Fig. 24).

To further confirm these findings, we performed gDNA-based sequencing of thymus and paired circulating prethymectomy blood specimens that were different from those examined by mRNA-based sequencing. These unique specimens were collected from three of the patients participating in the MGTX trial (SI Appendix, Fig. S7 and Table S2). We sequenced gDNA and identified shared B cell clones; the analysis of sharing and background sharing was then performed as above. Clonally related B cells residing in the thymus and circulation could be detected across all three patients. Specifically, we found 21 (0.93% of all thymus clones), 10 (0.31%), and 1 (0.06%) shared clones, respectively, for each of the three patients and an average background of 0.5 for each of the three patients (0.02%, 0.03%, and 0.02%, respectively) (Fig. 3). Thus, these data from specimens, examined using complementary sequencing approaches,

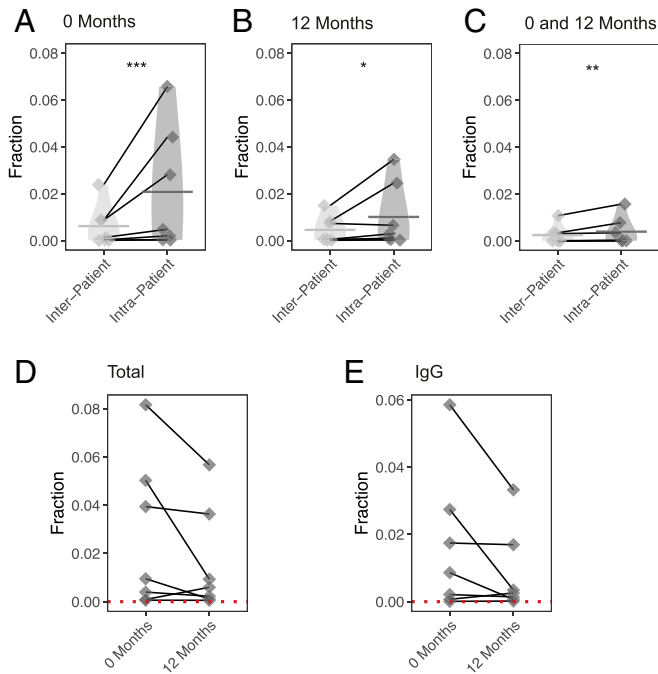
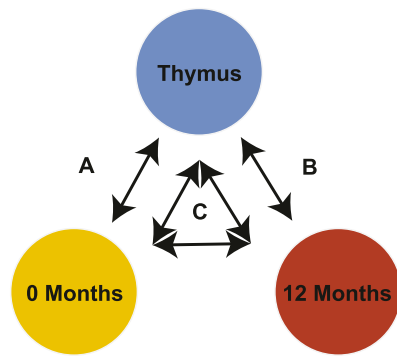


**Fig. 2.** B cell clones are shared between thymus and circulation before and 12 mo after thymectomy. An mRNA-based sequencing approach was used to evaluate how B cell clones are shared between the thymus and circulation before and 12 mo after thymectomy. The schematic diagram shows the corresponding computation of clonal sharing associated with each subpanel below. Clonal sharing is quantified as the number of shared clones divided by the number of clones in the corresponding thymus repertoire (or background thymus repertoire). This is shown for the sharing of clones found in the thymus with (A) clones found in prethymectomy circulation, (B) the postthymectomy circulation samples, and also (C) clones shared between the pre- and postthymectomy circulation samples. The change in sharing per patient is also shown before and after thymectomy (D) for both the total repertoire and (E) for the repertoire filtered only for IgG-switched V(D)J sequences. Quantification of clonal sharing from the same patient is paired with a gray line. Statistical differences are shown only when significant ( $***P < 0.001$ ;  $**P < 0.01$ ;  $*P < 0.05$ ).

collectively demonstrate that a fraction of B cell clones residing in the thymus can also be found in the circulation prior to thymectomy.

**B Cell Clones Shared between the Thymus and Circulation Feature a Distinct Repertoire.** We speculated that B cells in the circulation belonging to clones shared with the thymus display the features that are characteristic of thymus-resident B cells: Specifically, that they are more clonally expanded, more frequently class-switched to IgG, and have accumulated more SHM than those

that are not shared with the thymus. Therefore, we investigated these features among clones shared between the thymus and circulation. We first tested the hypothesis that B cells found in the circulation that are shared with the thymus (referred to as “thymus-associated”) are clonally expanded to a greater extent, given that antibody-secreting cells and B cells responding to antigen typically have this characteristic. Clones in the circulation shared with the thymus were confirmed to be more clonally expanded (larger clone size) when compared to clones in the circulation that were not shared (paired  $t$  test  $P = 0.042$ ) (Fig. 4A).

We next investigated the overall isotype distribution of clones in the circulation shared with the thymus. Given that thymus-resident clones are disproportionately IgG-switched, we speculated that thymus-associated clones would also be more IgG-switched. A large fraction (41.3%) of circulating clones that were shared with the thymus were IgG-switched compared to only 27.8% of the clones that were not shared (paired  $t$  test  $P = 0.003$ ) (Fig. 4B). In comparison, there was no significant difference in the fraction of IgM- or IgA-switched V(D)J sequences among clones that were shared compared to those that were not shared.

We then tested if these IgG-switched B cell clones in the circulation, which are shared with the thymus, have higher frequencies of SHM compared to nonshared circulating clones, given our previous observation that IgG-switched B cells in the thymus are more mutated. The frequency of SHM among shared clones in the circulation was 6.3%, while the frequency among nonshared IgG-switched clones was 5.1%, (paired  $t$  test  $P = 0.024$ ) (Fig. 4C). No significant differences were observed in the SHM frequency of IgM and IgA clones that were shared with thymus repertoire compared to those that were not shared. These findings are also consistent with the possibility that B cells in the circulation belonging to clones shared with the thymus display features specific to thymus-resident B cells and may therefore have emigrated from the thymus.

**B Cell Clones Populating the Thymus Persist in the Circulation after Thymectomy.** We next sought to investigate the fate of circulating thymus-associated B cell clones after thymectomy. Thus, clones shared between the thymus (at baseline) and PBMCs collected 12 mo after thymus removal were examined. A mean of 245.7 (1.0% of all thymus clones) clones were shared between the thymus and postthymectomy circulation, while a mean of only 65.7 (0.046% of all thymus clones) clones could be found to be shared in the background (one-tailed paired  $t$  test  $P = 5.4e-4$ ) (Fig. 2B and *SI Appendix*, Fig. S6). We also investigated whether there was more sharing than expected between the thymus, prethymectomy circulation, and postthymectomy circulation. We observed a mean of 104 (0.40% of all thymus clones) clones shared in all three compartments, while only 32 (0.25% of all thymus clones) were found shared in the background (one-tailed paired  $t$  test  $P = 0.017$ ) (Fig. 2C and *SI Appendix*, Fig. S6).

Additionally, we closely examined shared clones containing shared mutations relative to their inferred germline sequences. Two such trees from two independent B cell clones, members of which occupy both the thymus tissue and circulation prior to and 12-mo postthymectomy, are shown as illustrative examples (*SI Appendix*, Figs. S8 and S9). These clonal variants (produced during the evolution of an immune response) are members of the same clone and contain many shared mutations, which are highly unlikely to arise by independent affinity maturation processes in separate tissues.

As a means to further validate the finding that thymus-resident clones persist in the circulation after thymectomy, we studied a patient (THY-Y) who underwent thymectomy at a tertiary care facility unaffiliated with the MGTX trial (Table 1). We tested for shared clones between the thymus and the circulation both prior

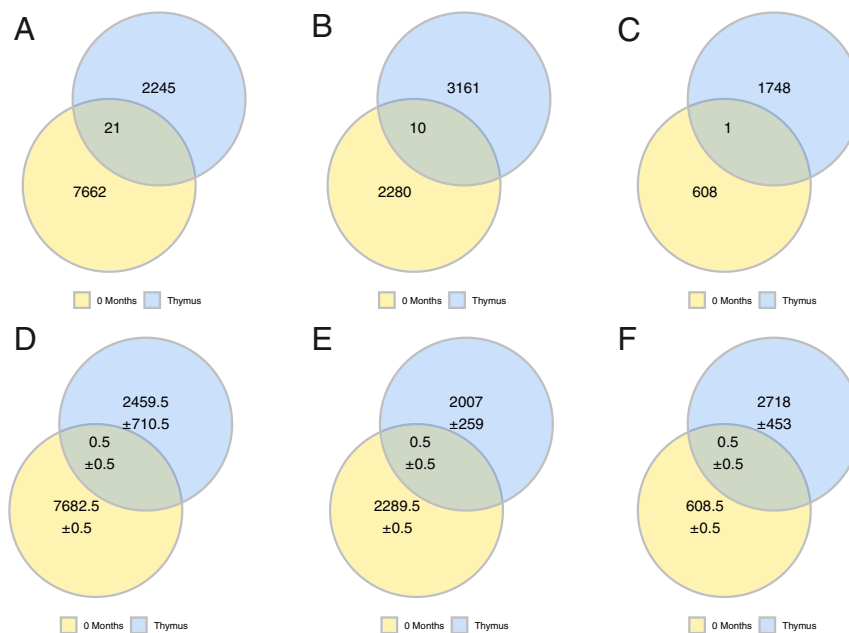


**Fig. 3.** B cell clones are shared between thymus and circulation before a thymectomy. A gDNA-based sequencing approach was used to confirm that B cell clones are shared between the thymus and circulation before thymectomy. The observed number of shared clones is shown for patient THY6 (A), patient THY7 (B), and patient THY2 (C). The computed background sharing is shown as Venn-diagrams for THY6 (D), patient THY7 (E), and patient THY2 (F). Background sharing was computed by changing the identity of the thymus used to assess for clonal sharing: That is, the observed sharing of clones from thymus samples derived from different patients with the circulation and computing an average. Uncertainty was computed as the SD of values from the corresponding background sharing and are shown in D–F using the “±” symbol.

to and at 6 mo after thymectomy. The number of shared clones prior to thymectomy (3,126 clones) and at 6 mo (660 clones) was more elevated than the background at those same time points (417.1 clones prior to thymectomy one-tail paired  $t$  test  $P = 5.4e-8$ ; 118.74 clones after thymectomy one-tail paired  $t$  test  $P = 3.4e-6$ ) (Fig. 5). Thus, these findings provide an independent MG confirmation that B cell clones populating the hyperplastic MG thymus can persist in the circulation following thymectomy.

Finally, we investigated whether the frequency of thymus-associated clones would decline over time as a consequence of thymectomy. The fraction of circulating thymus-associated clones (quantified in Fig. 2 A and B) prethymectomy and 12 mo post-thymectomy was examined. Five of seven patients showed a decline

in the frequency of thymus-associated clones in the circulation. (Fig. 2D). Moreover, for the same five of seven patients, a similar decline was observed when investigating only the IgG compartment (Fig. 2E). Thus, for most patients, thymus-associated B cell clones can persist at 12 mo after thymus removal. However, the fraction of these circulating clones generally declines after thymectomy although this is not consistently observed across all patients.

**Circulating Thymus-Associated B Cell Clones Initially Mature in the Thymus.** We next investigated whether shared clones showed evidence of movement from the thymus to the circulation by analyzing the lineage structure of these clones. Only IgG sequences from the thymus and circulation at the time of thymectomy were

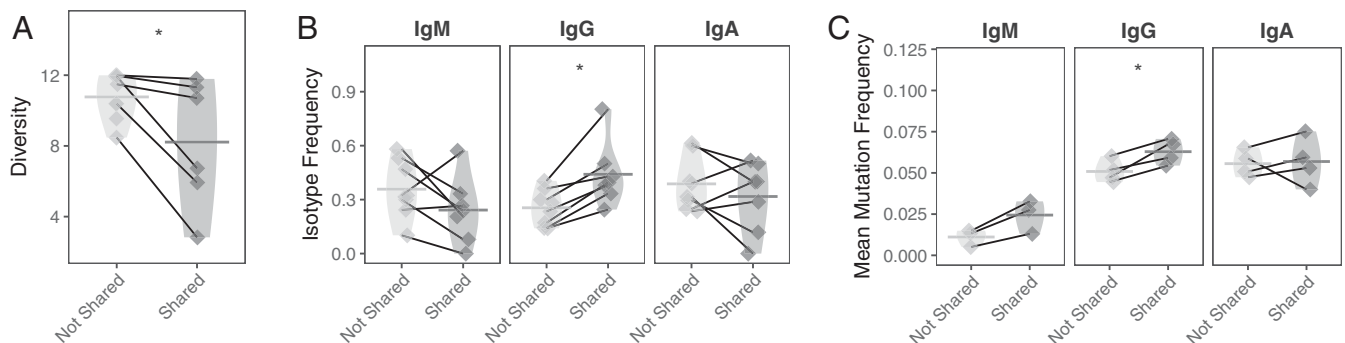


**Fig. 4.** Features of clones shared between the thymus and prethymectomy circulation are distinct from circulating clones that are not shared. (A) Simpson's diversity of shared prethymectomy and thymus clones in the circulation. Lower values of diversity correspond to greater clonal expansion; that is, circulating clones shared with the thymus are more clonally expanded than their nonshared circulating counterparts. Diversity values belonging to the same patient are paired with a gray line. (B) Usage of different isotypes among shared and nonshared clones is shown for IgM, IgG, and IgA for the circulating repertoire. Horizontal bars show the average isotype usage frequency for clones that are either shared or not shared. Frequencies belonging to the same patient are paired with a gray line. (C) Average SHM frequencies among shared and nonshared clones are shown for IgM, IgG, and IgA for the circulating repertoire. Horizontal bars show the average SHM frequency for a given cluster. Frequencies belonging to the same patient are paired with a gray line. Statistical differences are shown only when significant (\* $P < 0.05$ ).

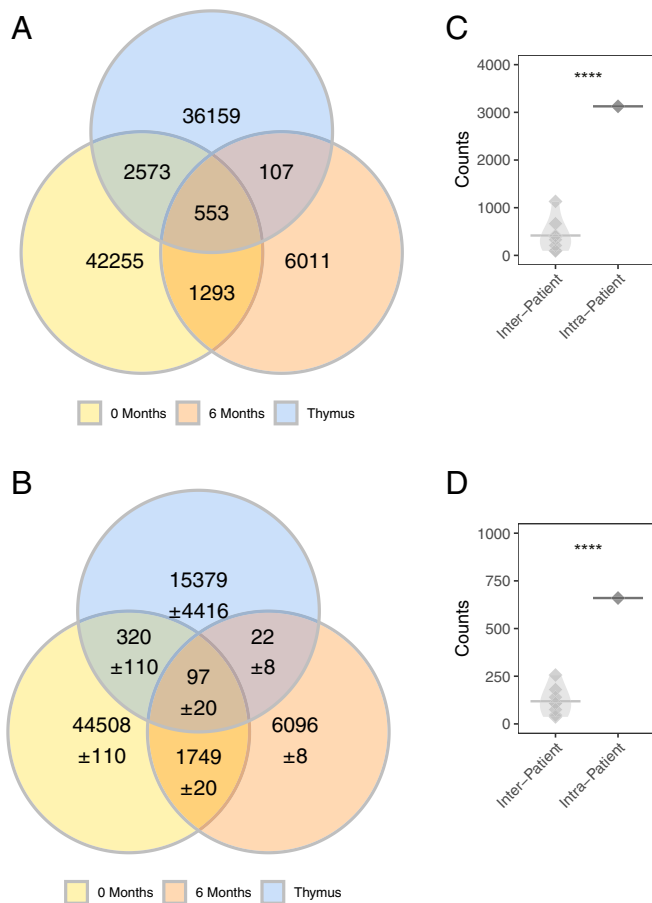


**Fig. 5.** Confirmation of B cell clonal sharing with the circulation in specimens (THY-Y) independent of the MGTX trial. (A) Observed number of clones shared between the prethymectomy, postthymectomy circulation, and thymus shown as Venn diagrams. (B) Computed background sharing between the prethymectomy, postthymectomy circulation and thymus are shown as Venn diagrams. Background sharing was computed by permuting the identity of the thymus used to assess for clonal sharing and computing an average; this approach is identical to the approach used to compute clonal sharing for thymus samples from the MGTX trial. Uncertainty was computed as the SD of the background clonal sharing and shown using the “±” symbol. Statistical testing of observed counts of shared clones between circulation and thymus repertoire (C) prethymectomy and (D) postthymectomy. Statistical differences are shown only when significant (\*\*\*\* $P < 0.0001$ ).

included in this analysis because of their importance in AChR autoantibody MG immunopathology. Given the location (thymus or circulation) associated with each tip of a lineage tree, we used a maximum parsimony algorithm (23) to determine the most parsimonious history of changes between thymus and circulation along the tree. The types of predicted changes that occurred within the trees of each repertoire were then compared to those obtained from the same trees with randomized tissue states (circulation or thymus) at the tips (60). Two patients (THY6 and THY7) showed a significantly greater proportion of predicted changes from thymus to circulation compared to randomized trees (both  $P = 0.01$ ) (SI Appendix, Table S3). Two patients (THY1 and THY2) showed a greater proportion of changes in the opposite direction—from circulation to thymus—but these did not reach significance ( $P = 0.37$  and  $0.17$ , respectively). However, when analyzed as a group, the patients had a significantly greater proportion of predicted changes from thymus to circulation with a Fisher combined  $P$  value of  $0.014$ . These results suggest a biased ancestor/descendant relationship from the thymus to circulation

within the lineage trees of these patients. This relationship could theoretically be driven by undersampling of thymus sequences relative to circulation (60). However, between 1.9- and 260- (median = 2.7) fold more sequences were obtained from the thymus than circulation for the patients included (SI Appendix, Table S3). This suggests that undersampling of the thymus is unlikely. Rather, we reason that, after switching to IgG, these clones accumulated early somatic hypermutations in the thymus before migrating to circulation.

**Changes in the Frequency of Shared B Cell Clones Correlates with Measures of Clinical Outcome.** Associations between features of the B cell repertoire and clinical measurements were next explored. We specifically tested whether the change in the sharing of clones between the circulation and thymus correlated with clinical benefit from thymectomy by comparing the change in clonal sharing with measures of patient outcome available from the MGTX clinical trial (42). The primary outcomes of change in average quantitative MG (QMG) test score and change in average steroid dosage (in milligrams) were examined. Given that two patients were not treated with daily prednisone prior to the start of the trial (subjects THY3 and THY5) (Table 1), only the change in steroid dosage between years 1 and 2 (after concomitant steroid treatment has been started after thymectomy) could be examined. In comparison, the change in QMG score between baseline and year 1, and between year 1 and year 2 were both examined. To account for the different depths of sequencing from the blood and thymus samples, a Bray–Curtis index for sharing, which quantifies the number of clones shared between these two compartments as a fraction of the combined size of the two compartments, was computed. A Bray–Curtis index of 1 indicates that two sites share all of the same clones; an index of 0 indicates that no clones are shared. To express relative changes in sharing between the thymus and circulation, the (log) fold-change (comparing baseline and postthymectomy) in Bray–Curtis index between the two compartments was computed.

The association between change in total sharing with the change in QMG score was examined first. A significant positive correlation of  $0.727$  was observed ( $P = 0.032$ ), showing that increased clonal sharing between 0 and 12 mo is associated with increases in QMG score and therefore a worsening clinical outcome, while decreased clonal sharing is associated with decreased QMG score and better clinical outcomes (Fig. 6A). However, no correlation was found between the change in QMG score between baseline (prethymectomy) and year 1 with the change in clonal sharing ( $-0.024$ ,  $P = 0.521$ ) (Fig. 6B). Next, the change in total clonal sharing with the change in prednisone dose was quantified between years 1 and 2. A significant correlation of  $0.874$  was observed ( $P = 0.005$ ) showing that increases in clonal sharing are associated with increases in steroid requirements needed to control symptoms (Fig. 6C). Similar associations were detected when restricting the analysis to IgG-switched B cell clonal sharing and clinical outcomes with a significant correlation observed between change in sharing and change in QMG score between years 1 and 2 ( $0.855$ ,  $P = 0.007$ ) (Fig. 6E), but not between baseline and year 1 ( $0.378$ ,  $P = 0.15$ ) (Fig. 6F); significant correlations were also observed for change in sharing and change in prednisone dose ( $0.688$ ,  $P = 0.044$ ) (Fig. 6G). Overall, patients from the trial who had fewer thymus B cell clones shared with the circulation after thymectomy had more favorable outcomes than those who had more thymus clones after thymectomy. This is well-illustrated by the findings derived from patient THY1, who responded poorly to thymectomy with an increase in QMG score between years 1 and 2 ( $+0.472$ , and also little change between baseline and years 1 to  $2.877$ ) and only a  $10.6$ -mg decline in steroid dose. This patient also had only a slight decrease in the sharing between clones from the resected thymus (log fold-decrease of  $-0.08$ , or a decrease of  $7.7\%$ ) and the

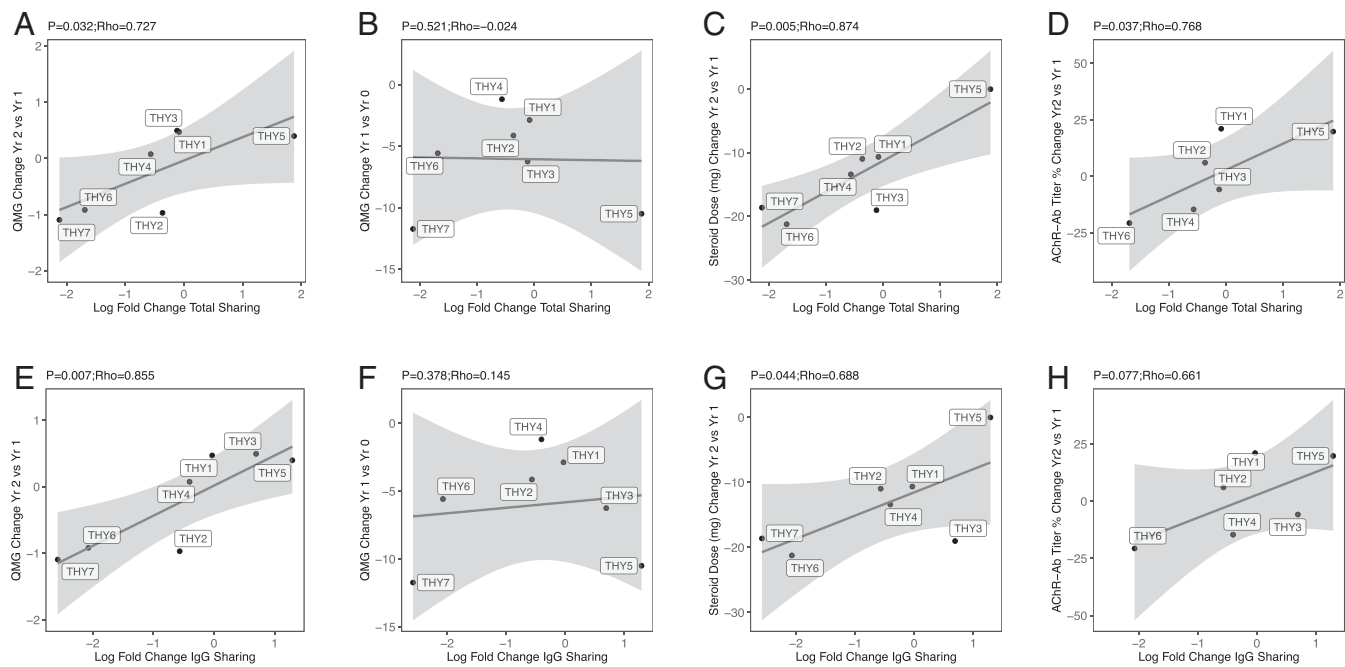


**Fig. 6.** Correlation between clinical outcome measurements and circulating thymus-associated B cells. Correlation of the log fold-change in clonal sharing between the thymus and circulation as assessed with a Bray–Curtis index (on the x axis) and with (A) the change in QMG score between years 1 and 2 after thymectomy, (B) the change in QMG score between baseline and year 1 after thymectomy, (C) the change in steroid dose between years 1 and 2 after thymectomy, and (D) the percentage change in AChR autoantibody titer between years 1 and 2 after thymectomy (on the y axis). The same analysis is shown for the log fold-change in IgG clonal sharing (E–H), respectively. AChR autoantibody titer was not collected for THY7 (D and H).

circulating repertoire. In comparison, both patient THY6 and THY7 performed well in terms of change in QMG score (−0.917 and −1.093, respectively) and steroid dosage (−21.2 mg and −18.6 mg, respectively). These patients had decreases in clonal sharing between the circulation and the thymus after thymectomy (log fold-change of −2.031 or 86.9% and −2.753 or 93.6%, respectively). Thus, smaller decreases (or even no decrease) in clonal sharing between the circulation and thymus may be associated with poor outcomes in terms of long-term changes in steroid dose and QMG score between years 1 and 2 but not between baseline and year 1, that is, immediately after surgery.

Associations with AChR autoantibody titer were available for six patients. The change in clonal sharing was compared to the percent change in AChR autoantibody titer between years 1 and 2, as the change in clonal sharing was also observed to correlate with change in QMG and steroid use during this time period. A significant correlation was observed when examining the total immunoglobulin repertoire ( $P = 0.037$ ) (Fig. 6D); however, no significant correlation was observed when examining the IgG-switched repertoire ( $P = 0.077$ ) (Fig. 6H). To test if the persistence of clonal overlap would also depend on the accumulation of disease-relevant thymus B cells over time, the correlation between duration of disease prior to thymectomy and the persistence of these B cells was also examined. No significant correlations were observed with change in total immunoglobulin or IgG overlap (SI Appendix, Fig. S10). Thus, thymic B cell persistence may directly contribute to changes in elevated AChR autoantibody titers after thymectomy in some patients. However, this association is less clear than the direct correlation between persistence and symptoms.

## Discussion

Thymectomy was recently confirmed to be beneficial in a randomized clinical trial setting (20, 42, 43). While patients often improve following thymectomy, complete stable remission is

seldom achieved with surgery alone. The thymus is also a source of disease-causing AChR autoantibody-producing B cells. In this study, we test the hypothesis that circulating B cell clones can be traced to thymus B cell clones, including plasma cells, and that the persistence of these clones is associated with poor disease outcomes. By testing this hypothesis, which has not been previously investigated, we can potentially show that B cell clones in the periphery of patients with AChR-MG persist and could contribute to poor disease outcomes. We formally tested this hypothetical model by applying AIRR-seq approaches, which can identify rare disease-related sequences in the large ( $10^{11}$  B cells) circulating peripheral B cell gene repertoire found in humans (67). By broadly sequencing the B cell receptors of thymus B cells, we found that: 1) Thymus-associated B cell clones persist in the circulation long after thymectomy, which was demonstrated using two complementary approaches and independent sets of samples; 2) shared clones (those found in both the circulation and thymus) were IgG-switched, displayed a high frequency of accumulated SHM, including those generating N-glycosylation sites, all of which are features consistent with an antigen-driven response; 3) clonal family trees showed that a disproportionate frequency of these clones originated from the thymus, suggesting that they accumulated mutations in the thymus before migrating to the circulation; and 4) an increased frequency of persistent clones showed a positive association with a worse disease status after the treatment, and 5) was associated with changes in AChR autoantibody titers in some patients. These findings provide key insights into the mechanisms of MG immunopathology and the association between residual thymus-associated B cell populations and poor outcomes after thymectomy.

We employed a number of steps to ensure rigorous data collection. First, we used both gDNA and RNA for the sequencing template. DNA and RNA were isolated from whole blood as part of the MGTX trial. These specimens were collected and processed at a site separate from our laboratory. Furthermore,

the DNA-based and RNA-based sequencing were performed at separate sites. DNA specimens were sent to a commercial sequencing organization. Raw sequencing data were returned and analyzed by us. RNA specimens were sequenced and analyzed in-house. Finally, we studied a thymus specimen and matched PBMCs (time 0 and 6 mo) collected at an institution outside the MGTX trial, and the analysis of these specimens was completely independent of those from the trial. The collective data derived from these independent specimens and multiple approaches all provide results consistent with each other, and consistent with overall interpretations regarding persistent B cell clones postthymectomy.

Our findings suggest that B cell clones frequently accumulate ancestral mutations in the thymus before emigrating to the periphery. This indicates that the thymus may be the site in which these autoreactive B cells originate and mature. Their origin in the thymus is supported by a number of studies that highlight MG thymus resident cell populations as essential for the initiation and maintenance of autoantibody production. The MG thymus includes myoid cells that express AChR (33) and proinflammatory cytokines. Moreover, MHC class I<sup>+</sup> and class II<sup>+</sup> medullary thymic epithelial cells (mTEC) express AChR subunits (68) and are recognized by both autoantibodies (69) and complement (70) in the thymus. These mTECs play a role in priming and activating AChR-specific T cells. These T cell subsets include thymic-resident regulatory T cells (Tregs) that are defective in their ability to control autoimmune responses (71, 72) and, importantly, CD4<sup>+</sup> helper T cells that could activate antigen-specific B cells (73). Together, these T cell populations are key components of germinal centers that produce mature AChR-specific B cells and defective Tregs that contribute to perpetuating an abnormal response. Removal of the thymus would also remove these disease-relevant non-B cell subsets. Given their fundamental role in the autoimmune response, the diminished presence of these cell subsets is likely to also play a role in disease outcome following resection.

Exploratory examinations of potential clinical correlates were performed to broadly determine whether the frequency of circulating thymus-associated B cell clones associated with disease severity and treatment outcome. We observed an association between the steroid dose that was required to control disease and the change in clonal sharing of thymus-associated B cell clones for patients involved in the MGTX 2-y extension. This longer-term observational period was required to reach statistical significance. This finding supports the hypothesis that thymectomy reduces the frequency of circulating thymus-associated clones and that this beneficial effect may require considerable time to manifest. This is congruent with other studies that suggest that the thymus is the origin of autoantibody-producing clones, and serves to maintain these subsets during the course of disease (32, 74, 75). However, poor correlation between the change in clonal sharing and the change in QMG score was observed over the first year. We speculate that this reflects the possibility that the persistence of thymus B cells and plasma cells does not correlate with immediate treatment response after the surgery, but rather with more long-term outcomes. We also caution against interpreting changes in the persistence of thymus B cells in the circulation for the patient unaffiliated with the MGTX trial. The time after thymectomy when clonal overlap was assessed was shorter (6 mo) for this patient compared to the trial (12 mo) and it is not clear if changes in overlap are interpretable at this time point. Finally, no correlation was observed with change in clonal overlap and disease duration prior to thymectomy. This suggests that the accumulation of AChR autoantibody-specific B cells in the thymus may not be directly associated with duration of disease prior to thymectomy.

With new details provided by this study, we propose an updated speculative mechanism describing the immunopathology of AChR

autoantibody-positive MG involving thymic lymphofollicular hyperplasia. Immune dysregulation, a hallmark of autoimmunity, occurs during B cell development. B cells, developing in the bone marrow, include an elevated fraction of self-reactive cells due to B cell tolerance checkpoints, which are known to be defective in MG (76). This population of naïve B cells, which avoided counterselection, has been shown to serve as precursors to mature autoreactive B cells in other autoimmune settings and may play a similar role in MG (77). These naïve B cells encounter AChR antigens in the thymus presented by TECs and also receive T cell help; they then differentiate into memory B cells and autoantibody-secreting cells. These autoreactive B cell populations can remain in the thymus, most likely as residents of structures that resemble germinal centers that are characteristic of thymic lymphoid hyperplasia. These B cells then migrate from the thymus and populate other compartments. Clonal relatives of thymic emigrants, as shown here, can be found in the circulation. In addition, AChR autoantibody-producing cells are known to populate peripheral tissue compartments; specifically, they have been found in the circulation, lymph nodes, and bone marrow (29, 73, 78–80). While thymectomy will remove a large fraction of thymus-resident autoreactive B cells, plasma cells, and the cells that support their development, this treatment is performed only once the disease is established. This may be too late to halt disease progression, as those thymic B cells that have emigrated contribute to ongoing disease.

Our study included patients with extensive clinical documentation, given their enrollment in the MGTX trial. However, we recognize the limited number of patients included in the present study and thus encourage caution in generalizing our findings. The investigation nevertheless provides further support for the benefits of thymectomy and provides details regarding the mechanism of the disease immunopathology. The clinical correlations should be explored in larger studies. We did not observe persistent thymus-associated clones in all of the patients studied. This, in our view, could be attributed to limited sequencing depth in some of the specimens. We find that thorough characterization of the circulating repertoire requires sequencing unmanipulated PBMCs in the 1 to 4 × 10<sup>7</sup> total cell range; specimens of such size were not available from the MGTX trial (65). This point is highlighted by the study of the sample that was collected at our institution, from which we acquired remarkable sequencing depth from a large number of PBMCs. However, we leave open the possibility that in a subset of patients, thymus resident B cell clones do not reside outside of that tissue and do not persist in the circulation following surgical resection.

While our study leveraged a well-established computational platform for the identification of B cell clones from AIRR-seq data, precise identification of clones is not without limitations. Identifying clones in separate tissues can be confounded by errors associated with misidentification of similar sequences that arise out of V(D)J recombination generated with similar (or identical) IGH gene segments. Clonal relationships can be reliably inferred from IGH V(D)J sequences based on our previous studies, but this is a statistical procedure and false-positive relationships do occur (54).

Questions remain concerning postthymectomy therapeutic strategies and thymic-resident B cell phenotypes. While thymectomy removes a source of autoantibody-producing B cells, those that have emigrated from the thymus may continue to contribute to disease, particularly those that have already fully differentiated into plasma cells. This is supported by evidence from investigations of plasma cells from nonthymus sources, such as the bone marrow in patients with AChR-MG (79, 80). Combination therapies aimed at targeting residual thymus-associated B cells may prove to be a valuable part of a potential therapeutic strategy. The use of B cell-depleting agents, such as rituximab—which is currently used for the treatment of MG—fits this approach

well (81–83). Nevertheless, several groups have shown that patients with a different subtype of MG (MuSK) lacking thymic abnormalities respond more consistently to B cell-depletion therapy with rituximab than patients with AChR-MG, consistent with the resistance of disease-causing, tissue-resident, plasma cell-like B cell subsets (lacking surface CD20) in AChR-MG compared to MuSK MG (81–83). Thus, consideration may also be given to anti-CD19–based treatments that would specifically target plasma cells thought to be spared by rituximab (84). AIRR-seq approaches employed in this study do not distinguish plasma cells from B cells; the relative importance of these two subsets is unclear. While thymic plasma cells spontaneously produce AChR autoantibodies, their CD20<sup>+</sup> germinal center B cell counterparts also possess AChR reactivity and the frequency of germinal centers associates with disease severity and AChR autoantibody titer (27, 34, 36). Thus, although plasma cells are known to play an important role in the etiology of AChR-MG through the production of AChR autoantibodies, CD20<sup>+</sup> B cells also appear to make contributions to disease pathogenesis.

Combining our approach with single-cell transcriptome and simultaneous paired repertoire techniques would afford the characterization of the transcriptomes of these B cell populations. These studies would also afford the production and testing of recombinant monoclonal antibodies for AChR binding and pathogenic capacity from thymus-associated B cells. Additionally, thymus B cells are not all AChR-specific (29, 37). The B cell receptors we found in the thymus were nearly 100% antigen experienced and are likely to also target exogenous (e.g., infection or vaccination related) and perhaps self-antigens (29, 85). Provided that these disease-relevant cells had unique and

identifiable transcriptional characteristics, they could also serve as valuable biomarkers for monitoring MG disease progress. Diagnostic algorithms incorporating thymus imaging after thymectomy and BCR repertoire evaluation may provide a means to assess the potential need for surgical re-exploration versus further immunotherapy. Thus, tracking the persistence of thymic-derived B cells after therapy may represent an invaluable biomarker for the management of patients with AChR-MG.

**Data Availability.** The data reported in this paper have been deposited in the National Center for Biotechnology Information Sequence Read Archive, <https://www.ncbi.nlm.nih.gov/sra> (BioProject ID PRJNA658100). Code used in this study is available in a publicly accessible repository at <https://bitbucket.org/kleinsteinst/projects>.

**ACKNOWLEDGMENTS.** We thank Karen Boss for providing editorial assistance; Jonathan Marquez for providing reagents for the purification of whole-blood RNA from the MGTX trial used in this study; Lisa Gras and Aditya Kumar for assisting with the collection of thymus samples; Abeer Obaid and Soumya Yandamuri for careful reading and editing of the manuscript; and Drs. Eileen Dimalanta and Chen Song from New England Biolabs for providing reagents used for the preparation of bulk B cell receptor libraries. This project was supported by the National Institute of Allergy and Infectious Diseases (NIAID) through Grants R01-AI114780 and R21-AI142198 (to K.C.O.), and R01-AI104739 (to S.H.K.); National Institute of Neurological Disorders and Stroke Grant U01-NS042685 (to H.J.K. and I.A.); and Muscular Dystrophy Association Neuromuscular Disease Research program Award MDA575198 (to K.C.O.). R.J. is supported by NIAID Award F31-AI154799). K.B.H. was supported through a PhRMA Foundation postdoctoral fellowship in Informatics.

1. A. Vincent, Unravelling the pathogenesis of myasthenia gravis. *Nat. Rev. Immunol.* **2**, 797–804 (2002).
2. N. E. Gilhus *et al.*, Myasthenia gravis—Autoantibody characteristics and their implications for therapy. *Nat. Rev. Neurol.* **12**, 259–268 (2016).
3. J. M. Lindstrom, A. G. Engel, M. E. Seybold, V. A. Lennon, E. H. Lambert, Pathological mechanisms in experimental autoimmune myasthenia gravis. II. Passive transfer of experimental autoimmune myasthenia gravis in rats with anti-acetylcholine receptor antibodies. *J. Exp. Med.* **144**, 739–753 (1976).
4. K. Oda, S. Korenaga, Y. Ito, Myasthenia gravis: Passive transfer to mice of antibody to human and mouse acetylcholine receptor. *Neurology* **31**, 282–287 (1981).
5. R. Sterz *et al.*, Effector mechanisms in myasthenia gravis: End-plate function after passive transfer of IgG, Fab, and F(ab')<sub>2</sub> hybrid molecules. *Muscle Nerve* **9**, 306–312 (1986).
6. S. Viegas *et al.*, Passive and active immunization models of MuSK-Ab positive myasthenia: Electrophysiological evidence for pre and postsynaptic defects. *Exp. Neurol.* **234**, 506–512 (2012).
7. K. Tokya, D. Brachman, A. Pestronk, I. Kao, Myasthenia gravis: Passive transfer from man to mouse. *Science* **190**, 397–399 (1975).
8. J. O. Donaldson *et al.*, Antiacetylcholine receptor antibody in neonatal myasthenia gravis. *Am. J. Dis. Child.* **135**, 222–226 (1981).
9. D. Melber, Maternal-fetal transmission of myasthenia gravis with acetylcholine receptor antibody. *N. Engl. J. Med.* **318**, 996 (1988).
10. C. LePrince *et al.*, Thymic B cells from myasthenia gravis patients are activated B cells. Phenotypic and functional analysis. *J. Immunol.* **145**, 2115–2122 (1990).
11. A. K. Lefvert, S. Cuénoud, B. W. Fulpius, Binding properties and subclass distribution of anti-acetylcholine receptor antibodies in myasthenia gravis. *J. Neuroimmunol.* **1**, 125–135 (1981).
12. S. Nakano, A. G. Engel, Myasthenia gravis: Quantitative immunocytochemical analysis of inflammatory cells and detection of complement membrane attack complex at the end-plate in 30 patients. *Neurology* **43**, 1167–1172 (1993).
13. A. Rødgaard, F. C. Nielsen, R. Djurup, F. Somnier, S. Gammeltoft, Acetylcholine receptor antibody in myasthenia gravis: Predominance of IgG subclasses 1 and 3. *Clin. Exp. Immunol.* **67**, 82–88 (1987).
14. A. G. Engel, J. M. Lindstrom, E. H. Lambert, V. A. Lennon, Ultrastructural localization of the acetylcholine receptor in myasthenia gravis and in its experimental autoimmune model. *Neurology* **27**, 307–315 (1977).
15. H. Hara *et al.*, Detection and characterization of blocking-type anti-acetylcholine receptor antibodies in sera from patients with myasthenia gravis. *Clin. Chem.* **39**, 2053–2057 (1993).
16. P. J. Whiting, A. Vincent, J. Newsom-Davis, Acetylcholine receptor antibody characteristics in myasthenia gravis. Fractionation of  $\alpha$ -bungarotoxin binding site antibodies and their relationship to IgG subclass. *J. Neuroimmunol.* **5**, 1–9 (1983).
17. R. R. Almon, C. G. Andrew, S. H. Appel, Serum globulin in myasthenia gravis: Inhibition of  $\alpha$ -bungarotoxin binding to acetylcholine receptors. *Science* **186**, 55–57 (1974).
18. H. Loutrari, A. Kokla, S. J. Tzartos, Passive transfer of experimental myasthenia gravis via antigenic modulation of acetylcholine receptor. *Eur. J. Immunol.* **22**, 2449–2452 (1992).
19. D. B. Drachman, C. W. Angus, R. N. Adams, J. D. Michelson, G. J. Hoffman, Myasthenic antibodies cross-link acetylcholine receptors to accelerate degradation. *N. Engl. J. Med.* **298**, 1116–1122 (1978).
20. C. A. Weis, B. Schalke, P. Ströbel, A. Marx, Challenging the current model of early-onset myasthenia gravis pathogenesis in the light of the MGTX trial and histological heterogeneity of thymectomy specimens. *Ann. N. Y. Acad. Sci.* **1413**, 82–91 (2018).
21. A. Meraouna *et al.*, The chemokine CXCL13 is a key molecule in autoimmune myasthenia gravis. *Blood* **108**, 432–440 (2006).
22. T. Mittag, P. Kornfeld, A. Tormay, C. Woo, Detection of anti-acetylcholine receptor factors in serum and thymus from patients with myasthenia gravis. *N. Engl. J. Med.* **294**, 691–694 (1976).
23. A. Vincent, Tissue-specific antibodies in myasthenia gravis. *J. Clin. Pathol. (Br. J. Clin. Pathol.)* **13**, 97–106 (1979).
24. S. Schönbeck, F. Padberg, R. Hohlfeld, H. Wekerle, Transplantation of thymic autoimmune microenvironment to severe combined immunodeficiency mice. A new model of myasthenia gravis. *J. Clin. Invest.* **90**, 245–250 (1992).
25. A. Vincent, G. K. Scadding, H. C. Thomas, J. Newsom-Davis, In-vitro synthesis of anti-acetylcholine-receptor antibody by thymic lymphocytes in myasthenia gravis. *Lancet* **1**, 305–307 (1978).
26. H. N. A. Willcox, J. Newsom-Davis, L. R. Calder, Cell types required for anti-acetylcholine receptor antibody synthesis by cultured thymocytes and blood lymphocytes in myasthenia gravis. *Clin. Exp. Immunol.* **58**, 97–106 (1984).
27. R. P. Lisak *et al.*, In vitro synthesis of antibodies to acetylcholine receptor by peripheral blood cells: Role of suppressor T cells in normal subjects. *Neurology* **34**, 802–805 (1984).
28. A. I. Levinson, B. Zweiman, R. P. Lisak, A. Dziarski, A. R. Moskowitz, Thymic B-cell activation in myasthenia gravis. *Neurology* **34**, 462–468 (1984).
29. R. P. Lisak, A. I. Levinson, B. Zweiman, M. J. Kornstein, Antibodies to acetylcholine receptor and tetanus toxoid: In vitro synthesis by thymic lymphocytes. *J. Immunol.* **137**, 1221–1225 (1986).
30. S. Berrih-Aknin, R. Le Panse, Myasthenia gravis: A comprehensive review of immune dysregulation and etiological mechanisms. *J. Autoimmun.* **52**, 90–100 (2014).
31. F. G. Staber, U. Fink, W. Sack, Letter: B lymphocytes in the thymus of patients with myasthenia gravis. *N. Engl. J. Med.* **292**, 1032–1033 (1975).
32. I. Roxanis, K. Mickle, J. McConville, J. Newsom-Davis, N. Willcox, Thymic myoid cells and germinal center formation in myasthenia gravis; possible roles in pathogenesis. *J. Neuroimmunol.* **125**, 185–197 (2002).
33. A. Marx *et al.*, The different roles of the thymus in the pathogenesis of the various myasthenia gravis subtypes. *Autoimmun. Rev.* **12**, 875–884 (2013).
34. M. Okumura *et al.*, The immunologic role of thymectomy in the treatment of myasthenia gravis: Implication of thymus-associated B-lymphocyte subset in reduction of the anti-acetylcholine receptor antibody titer. *J. Thorac. Cardiovasc. Surg.* **126**, 1922–1928 (2003).

35. G. P. Sims, H. Shiono, N. Willcox, D. I. Stott, Somatic hypermutation and selection of B cells in thymic germinal centers responding to acetylcholine receptor in myasthenia gravis. *J. Immunol.* **167**, 1935–1944 (2001).
36. K. Vrolix *et al.*, Clonal heterogeneity of thymic B cells from early-onset myasthenia gravis patients with antibodies against the acetylcholine receptor. *J. Autoimmun.* **52**, 101–112 (2014).
37. Y. F. Graus *et al.*, Human anti-nicotinic acetylcholine receptor recombinant Fab fragments isolated from thymus-derived phage display libraries from myasthenia gravis patients reflect predominant specificities in serum and block the action of pathogenic serum antibodies. *J. Immunol.* **158**, 1919–1929 (1997).
38. A. Cardona, O. Pritsch, G. Dumas, J. F. Bach, G. Dighiero, Evidence for an antigen-driven selection process in human autoantibodies against acetylcholine receptor. *Mol. Immunol.* **32**, 1215–1223 (1995).
39. J. Farrar *et al.*, Diverse Fab specific for acetylcholine receptor epitopes from a myasthenia gravis thymus combinatorial library. *Int. Immunol.* **9**, 1311–1318 (1997).
40. N. S. Zuckerman *et al.*, Ectopic GC in the thymus of myasthenia gravis patients show characteristics of normal GC. *Eur. J. Immunol.* **40**, 1150–1161 (2010).
41. W. Mi, N. J. Silvestri, G. I. Wolfe, A neurologist's perspective on thymectomy for myasthenia gravis: Current perspective and future trials. *Thorac. Surg. Clin.* **29**, 143–150 (2019).
42. G. I. Wolfe *et al.*; MGTX Study Group, Randomized trial of thymectomy in myasthenia gravis. *N. Engl. J. Med.* **375**, 511–522 (2016).
43. G. I. Wolfe *et al.*; MGTX Study Group, Long-term effect of thymectomy plus prednisone versus prednisone alone in patients with non-thymomatous myasthenia gravis: 2-year extension of the MGTX randomised trial. *Lancet Neurol.* **18**, 259–268 (2019).
44. S. Yu *et al.*, Eight-year follow-up of patients with myasthenia gravis after thymectomy. *Acta Neurol. Scand.* **131**, 94–101 (2015).
45. A. J. Kaufman *et al.*, Thymectomy for myasthenia gravis: Complete stable remission and associated prognostic factors in over 1000 cases. *Semin. Thorac. Cardiovasc. Surg.* **28**, 561–568 (2016).
46. A. Vincent, J. Newsom-Davis, P. Newton, N. Beck, Acetylcholine receptor antibody and clinical response to thymectomy in myasthenia gravis. *Neurology* **33**, 1276–1282 (1983).
47. H. Kim, Y. M. Lim, E. J. Lee, Y. J. Oh, K. K. Kim, Factors predicting remission in thymectomized patients with acetylcholine receptor antibody-positive myasthenia gravis. *Muscle Nerve* **58**, 796–800 (2018).
48. J. Glanville *et al.*, Naive antibody gene-segment frequencies are heritable and unaltered by chronic lymphocyte ablation. *Proc. Natl. Acad. Sci. U.S.A.* **108**, 20066–20071 (2011).
49. R. Jiang *et al.*, Single-cell repertoire tracing identifies rituximab-resistant B cells during myasthenia gravis relapses. *JCI Insight* **5**, e136471 (2020).
50. R. C. Edgar, MUSCLE: Multiple sequence alignment with high accuracy and high throughput. *Nucleic Acids Res.* **32**, 1792–1797 (2004).
51. W. Li, A. Godzik, Cd-hit: A fast program for clustering and comparing large sets of protein or nucleotide sequences. *Bioinformatics* **22**, 1658–1659 (2006).
52. M. P. Lefranc, IMG2T, the international ImMunoGeneTics database. *Nucleic Acids Res.* **31**, 307–310 (2003).
53. J. Ye, N. Ma, T. L. Madden, J. M. Ostell, IgBLAST: An immunoglobulin variable domain sequence analysis tool. *Nucleic Acids Res.* **41**, W34–W40 (2013).
54. N. T. Gupta *et al.*, Hierarchical clustering can identify B cell clones with high confidence in Ig repertoire sequencing data. *J. Immunol.* **198**, 2489–2499 (2017).
55. R Core Team, R: A Language and Environment for Statistical Computing (R Foundation for Statistical Computing, Vienna, Austria, 2014), ([www.R-project.org/](http://www.R-project.org/)).
56. G. Yaari, M. Uduman, S. H. Kleinstein, Quantifying selection in high-throughput immunoglobulin sequencing data sets. *Nucleic Acids Res.* **40**, e134 (2012).
57. M. O. Hill, Diversity and evenness: A unifying notation and its consequences. *Ecol. Soc. Am.* **54**, 427–432 (2015).
58. J. P. Felsenstein, PHYLIP—Phylogeny inference package (version 3.2). *Cladistics* **5**, 164–166 (2004).
59. D. Sankoff, Minimal mutation trees. *SIAM J. Appl. Math.* **28**, 35–42 (1919).
60. K. B. Hoehn, O. G. Pybus, S. H. Kleinstein, Phylogenetic analysis of migration, differentiation, and class switching in B cells. [bioRxiv:10.1101/2020.05.30.124446](https://doi.org/10.1101/2020.05.30.124446) (7 July 2020).
61. K. B. Hoehn *et al.*, Repertoire-wide phylogenetic models of B cell molecular evolution reveal evolutionary signatures of aging and vaccination. *Proc. Natl. Acad. Sci. U.S.A.* **116**, 22664–22672 (2019).
62. K. A. Lloyd *et al.*, Variable domain N-linked glycosylation and negative surface charge are key features of monoclonal ACPA: Implications for B-cell selection. *Eur. J. Immunol.* **48**, 1030–1045 (2018).
63. N. Hamza *et al.*, Ig gene analysis reveals altered selective pressures on Ig-producing cells in parotid glands of primary Sjögren's syndrome patients. *J. Immunol.* **194**, 514–521 (2015).
64. T. B. van der Houwen *et al.*, Chronic signs of memory B cell activation in patients with Behçet's disease are partially restored by anti-tumour necrosis factor treatment. *Rheumatology (Oxford)* **56**, 134–144 (2017).
65. J. A. Vander Heiden *et al.*, Dysregulation of B cell repertoire formation in myasthenia gravis patients revealed through deep sequencing. *J. Immunol.* **198**, 1460–1473 (2017).
66. G. Yaari, J. I. C. Benichou, J. A. Vander Heiden, S. H. Kleinstein, Y. Louzoun, The mutation patterns in B cell Ig receptors reflect the influence of selection acting at multiple time scales. *Philos. Trans. B* **370**, 20140242 (2015).
67. J. Glanville *et al.*, Precise determination of the diversity of a combinatorial antibody library gives insight into the human immunoglobulin repertoire. *Proc. Natl. Acad. Sci. U.S.A.* **106**, 20216–20221 (2009).
68. S. Poëa-Guyon *et al.*, Effects of cytokines on acetylcholine receptor expression: Implications for myasthenia gravis. *J. Immunol.* **174**, 5941–5949 (2005).
69. D. Safar, C. Aimé, S. Cohen-Kaminsky, S. Berrih-Aknin, Antibodies to thymic epithelial cells in myasthenia gravis. *J. Neuroimmunol.* **35**, 101–110 (1991).
70. M. I. Leite *et al.*, Fewer thymic changes in MuSK antibody-positive than in MuSK antibody-negative MG. *Ann. Neurol.* **57**, 444–448 (2005).
71. A. Balandina, S. Lécart, P. Darteville, A. Saoudi, S. Berrih-Aknin, Functional defect of regulatory CD4(+)CD25+ T cells in the thymus of patients with autoimmune myasthenia gravis. *Blood* **105**, 735–741 (2005).
72. A. Gradolatto *et al.*, Both Treg cells and Tconv cells are defective in the myasthenia gravis thymus: Roles of IL-17 and TNF- $\alpha$ . *J. Autoimmun.* **52**, 53–63 (2014).
73. J. Newsom-davis, N. Willcox, G. Scadding, L. Calder, A. Vincent, AChR antibody synthesis by cultured lymphocytes in myasthenia gravis: Thymic and peripheral blood cell interactions. *Ann. N. Y. Acad. Sci.* **377**, 393–402 (1981).
74. H. Shiono *et al.*, Scenarios for autoimmunization of T and B cells in myasthenia gravis. *Ann. N. Y. Acad. Sci.* **998**, 237–256 (2003).
75. M. A. Cron *et al.*, Thymus involvement in early-onset myasthenia gravis. *Ann. N. Y. Acad. Sci.* **1412**, 137–145 (2018).
76. J.-Y. Lee *et al.*, Compromised fidelity of B-cell tolerance checkpoints in AChR and MuSK myasthenia gravis. *Ann. Clin. Transl. Neurol.* **3**, 443–454 (2016).
77. E. Cotzomi *et al.*, Early B cell tolerance defects in neuromyelitis optica favour anti-AQP4 autoantibody production. *Brain* **142**, 1598–1615 (2019).
78. Y. Fujii, Y. Monden, J. Hashimoto, K. Nakahara, Y. Kawashima, Acetylcholine receptor antibody-producing cells in thymus and lymph nodes in myasthenia gravis. *Clin. Immunol. Immunopathol.* **34**, 141–146 (1985).
79. Y. Fujii, Y. Monden, J. Hashimoto, K. Nakahara, Y. Kawashima, Acetylcholine receptor antibody production by bone marrow cells in a patient with myasthenia gravis. *Neurology* **35**, 577–579 (1985).
80. Y. Fujii *et al.*, Specific activation of lymphocytes against acetylcholine receptor in the thymus in myasthenia gravis. *J. Immunol.* **136**, 887–891 (1986).
81. R. J. Nowak, D. B. Dicapua, N. Zebardast, J. M. Goldstein, Response of patients with refractory myasthenia gravis to rituximab: A retrospective study. *Ther. Adv. Neurol. Disord.* **4**, 259–266 (2011).
82. K. R. Robeson *et al.*, Durability of the rituximab response in acetylcholine receptor autoantibody-positive myasthenia gravis. *JAMA Neurol.* **74**, 60–66 (2017).
83. I. Illa *et al.*, Sustained response to rituximab in anti-AChR and anti-MuSK positive myasthenia gravis patients. *J. Neuroimmunol.* **201–202**, 90–94 (2008).
84. B. A. C. Cree *et al.*, Placebo-controlled study in neuromyelitis optica—ethical and design considerations. *Mult. Scler.* **22**, 862–872 (2016).
85. L. S. Klavinskis, N. Willcox, J. S. Oxford, J. Newsom-Davis, Antiviral antibodies in myasthenia gravis. *Neurology* **35**, 1381–1384 (1985).